AGU PUBLICATIONS

JGR

Journal of Geophysical Research: Space Physics

RESEARCH ARTICLE

10.1002/2014JA019963

Key Points:
- Zonal plasma motions inside bubbles are different from ambient plasma motion
- Zonal plasma motions are similar inside bubbles and in the bottomside
- Deviation of the zonal bubble motion reflects the shear in the zonal flow

Correspondence to:
H. Kil,
hyosub.kil@jhuapl.edu

Citation:
Kil, H., W. K. Lee, Y.-S. Kwak, Y. Zhang, L. J. Paxton, and M. Milla (2014), The zonal motion of equatorial plasma bubbles relative to the background ionosphere, *J. Geophys. Res. Space Physics*, *119*, 5943–5950, doi:10.1002/2014JA019963.

Received 13 MAR 2014
Accepted 6 JUL 2014
Accepted article online 9 JUL 2014
Published online 24 JUL 2014

The zonal motion of equatorial plasma bubbles relative to the background ionosphere

Hyosub Kil[1], Woo Kyoung Lee[2], Young-Sil Kwak[2], Yongliang Zhang[1], Larry J. Paxton[1], and Marco Milla[3]

[1]The Johns Hopkins University Applied Physics Laboratory, Laurel, Maryland, USA, [2]Korea Astronomy and Space Science Institute, Daejeon, South Korea, [3]Radio Observatorio de Jicamarca, Instituto Geofísico del Perú, Lima, Peru

Abstract The zonal motions of plasmas inside equatorial plasma bubbles are different from those in the background ionosphere. The difference was explained in terms of the tilt of bubbles by recent studies, but observational evidence of this hypothesis has not yet been provided. We examine this hypothesis and, at the same time, look for an alternative explanation on the basis of the coincident satellite and radar observations over Jicamarca (11.95°S, 76.87°W) in Peru. In the observations at premidnight by the first Republic of China satellite (altitude: 600 km, inclination: 35°), plasmas inside bubbles drift westward relative to ambient plasmas. The same phenomenon is identified by radar observations. However, the relative westward plasma motions inside bubbles occur regardless of the tilt of bubbles, and therefore, the tilt is not the primary cause of the deviation of the plasma motions inside bubbles. The zonal plasma motions in the topside are characterized by systematic eastward drifts, whereas the zonal motions of plasmas in the bottomside backscatter layer show a mixture of eastward and westward drifts. The zonal plasma motions inside backscatter plumes resemble those in the bottomside backscatter layer. These observations indicate that plasmas inside bubbles maintain the properties of the zonal plasma motions in the bottomside where the bubbles originate. With this assumption, the deviation of the zonal motions of plasmas inside bubbles from those of ambient plasmas is understood in terms of the difference of the zonal plasma flows in the bottomside and topside.

1. Introduction

Our knowledge of the plasma motions in the equatorial *F* region relies on the observations of the incoherent scatter radar (ISR) at the Jicamarca Radio Observatory (JRO) (11.95°S, 76.87°W) in Peru. Typically, the plasma motions are upward and westward during daytime and downward and eastward at night [e.g., *Fejer et al.*, 1991]. In situ satellite observations show the existence of a similar diurnal drift pattern in other longitudes [e.g., *Coley and Heelis*, 1989; *Fejer et al.*, 1995, 2008; *Kil et al.*, 2009; *Scherliess and Fejer*, 1999]. The ISR and in situ satellite observations provide the plasma motions at all local times (LTs). However, the ISR observations are available only for a few days in a month and the in situ satellite observations are not available continuously at a local region. In addition to the ISR and in situ satellite observations, the phenomenon known as "bubble" has been used as a tool for measuring the zonal plasma motion at night [*Abdu et al.*, 1985, 1987; *Basu et al.*, 1991, 1996; *Bhattacharyya et al.*, 2001; *de Paula et al.*, 2010; *Immel et al.*, 2003; *Kil et al.*, 2000, 2002; *Liu et al.*, 2013; *Makela*, 2006; *Martinis et al.*, 2003; *Park et al.*, 2007; *Sobral and Abdu*, 1990; *Valladares et al.*, 1996]. Bubbles indicate the structures or regions in which the plasma density is smaller than the ambient plasma density. The low plasma density inside a bubble is associated with the transport of low-density plasmas in the bottomside *F* region into a higher-altitude region. The formation of a steep plasma density gradient in the bottomside and the occurrence of upward plasma motions just after sunset provide a favorable condition for the creation of bubbles by the Rayleigh-Taylor instability [*Kelley*, 1989; *Sultan*, 1996]. Bubbles appear as nightglow suppressions in optical observations [e.g., *Makela*, 2006], and the electron density irregularities inside bubbles produce radio scintillation [e.g., *Basu and Basu*, 1981] and coherent backscattering [e.g., *Woodman and La Hoz*, 1976]. The zonal plasma motions are derived from those observations.

Bubbles have been used as tracers of the zonal motion of the bubble-embedded background ionosphere. However, differences exist between the plasma motions inside bubbles and in the background ionosphere [e.g., *Huang et al.*, 2010; *Kudeki and Bhattacharyya*, 1999]. Recent studies [*Huang et al.*, 2010; *Liu et al.*, 2013] explained the difference in terms of the tilt of bubbles. Following this hypothesis, the zonal drift of plasmas inside a bubble relative to the background ionosphere is westward when the bubble is tilted westward and eastward when the bubble is tilted eastward. The relative westward or eastward plasma motions inside a tilted

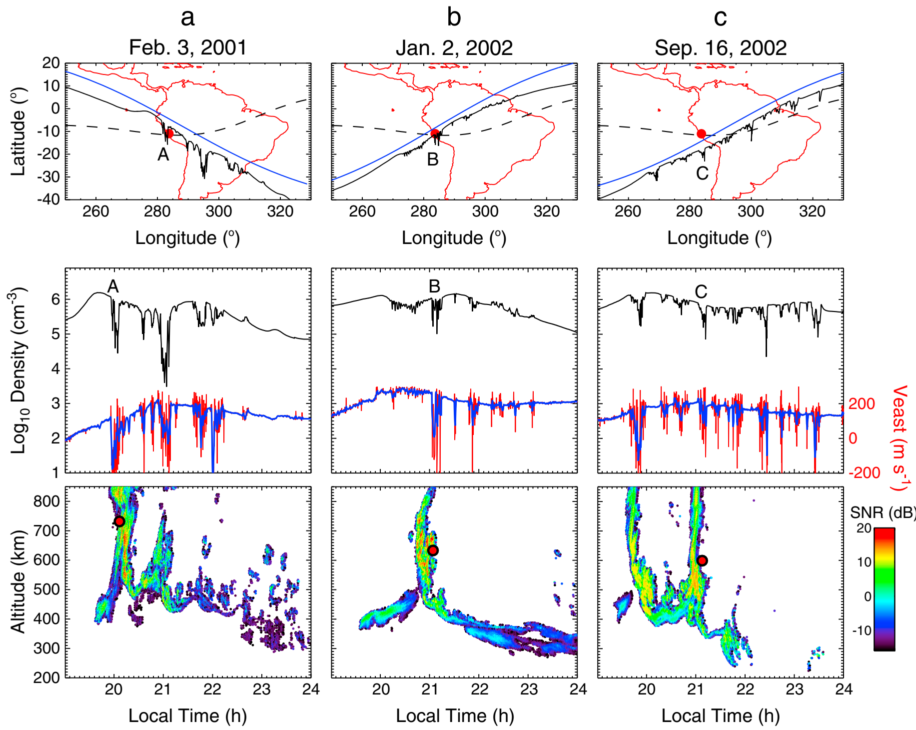

Figure 1. The ROCSAT-1 and JULIA observations on (a) 3 February 2001, (b) 2 January 2002, and (c) 16 September 2002. (top row) The ROCSAT-1 orbits (blue lines), (middle row) the ROCSAT-1 observations of plasma density (black lines) and zonal plasma velocity (red lines), and (bottom row) the JULIA observations of the backscatter powers. In Figure 1 (top row), the magnetic equator is shown by a black dashed line. In Figure 1 (middle row), the blue thick curves over the red curves are the five-point averaged zonal velocities. The magnetic apex heights of ROCSAT-1 orbits are shown by red dots.

bubble were explained by the polarization electric field induced by the plasma density gradient between the bubble and background ionosphere [*Huang et al*., 2010]. However, the deviation of the zonal plasma motions inside bubbles exists regardless of the tilt of bubbles in radar observations [e.g., *Kudeki and Bhattacharyya*, 1999]. From our own investigation of radar observations, we found that the fluctuations in the zonal plasma velocity are comparable to or even greater than the fluctuations in the vertical plasma velocity inside upright bubbles. The large fluctuations in the zonal plasma velocity inside upright bubbles are difficult to explain by the polarization electric field described above because the vertical component of the polarization electric field that drives the zonal plasma motion is zero inside an upright bubble. These observations raise a question about the hypothesis described above.

In this study, we provide an alternate explanation for the plasma motions inside bubbles based on the simultaneous satellite and radar observations. We also examine the hypothesis described above. *Huang et al*. [2010] validated their hypothesis using model simulation results, but the hypothesis has not yet been validated by observations. From the observations of the first Republic of China satellite (ROCSAT-1) (altitude: 600 km, inclination: 35°) [*Yeh et al*., 1999] from March 1999 to June 2004, we have searched for bubbles over JRO on the days when either the observations from the ISR or the 50 MHz coherent scatter radar, Jicamarca Unattended Long-term Investigations of the Ionosphere and Atmosphere (JULIA) [*Hysell and Burcham*, 1998], are available. We have found six events, and we report those events here.

2. Observations

2.1. Comparison of the ROCSAT-1 and JULIA Observations

The coincident observations of bubbles by ROCSAT-1 and JULIA occurred on 3 February 2001, 2 January 2002, 16 September 2002, and 2 October 2002. Bubbles were detected at premidnight on the first 3 days and at postmidnight on the last day. The ROCSAT-1 and JULIA observations at premidnight are shown in Figure 1: (a) 3 February 2001, (b) 2 January 2002, and (c) 16 September 2002. On each day, the ROCSAT-1 orbit (blue line),

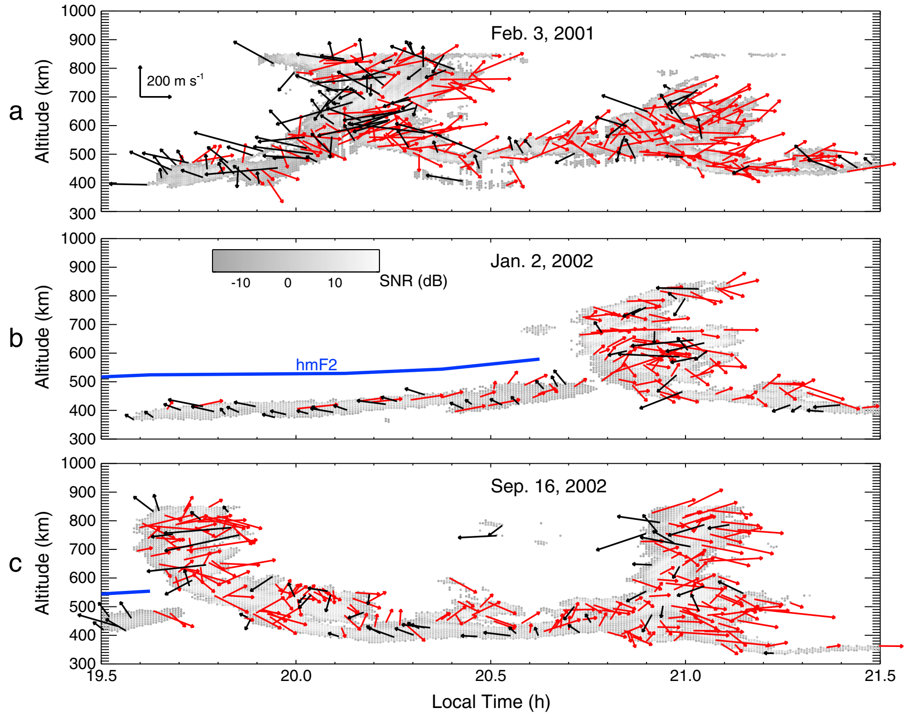

Figure 2. The JULIA observations of the plasma velocities on (a) 3 February 2001, (b) 2 January 2002, and (c) 16 September 2002. The westward and eastward plasma motions are distinguished by the black and red arrows, respectively. The hmF2 is shown by thick blue lines in Figures 2b and 2c.

ROCSAT-1 observations of plasma density (black line) and zonal plasma velocity (red line), and JULIA observation of the backscatter power (signal-to-noise ratio (SNR)) are shown from the top to the bottom. The magnetic equator is shown by a black dashed line in the map. The ROCSAT-1 observations are 1 s averaged data. In the middle panels, the blue thick curves over the red curves are the five-point averaged zonal velocities. The bubbles detected over JRO are marked by the letters "A," "B," and "C." The ROCSAT-1 orbits projected onto the magnetic equator along the magnetic field lines (magnetic apex heights) are shown with red dots in the SNR maps. Note that only those labeled bubbles match the plumes (vertical structures in the radar observations) at the same LTs. Backscatter plumes are produced by the electron density irregularities inside bubbles.

In the ROCSAT-1 observations, the zonal motions of plasmas in the background ionosphere (ionosphere where bubbles are absent) are steady eastward drifts. However, the plasma motions inside bubbles are turbulent. On average, as the thick blue curves show, the plasma motions inside bubbles are westward relative to the background ionosphere. The JULIA observations show that the bubbles labeled A, B, and C are associated with nearly upright plumes. We can estimate the tilt angles of the plumes by calculating the horizontal drift distance. With the use of the eastward drift velocity (~200 m s^{-1}) of the background ionosphere observed by ROCSAT-1, the tilt angles of plumes A, B, and C are approximately 18°, 0°, and 10°, respectively. *Huang et al.* [2010] explained the relative westward plasma motions inside bubbles in terms of the tilt of bubbles, but our observations show that the relative westward plasma motions occur at nearly upright plumes.

Figure 2 provides the JULIA observations of the plasma motions on (a) 3 February 2001, (b) 2 January 2002, and (c) 16 September 2002. The westward and eastward plasma motions are distinguished by the black and red arrows, respectively. In the figures hereafter, absolute velocities less than 50 m s^{-1} or greater than 500 m s^{-1} were not shown to minimize clutter. In the observation on 3 February 2001 (Figure 2a), the zonal plasma motions vary with LT; the westward motions are dominant before 19.8 LT, the westward and eastward motions are mixed at 19.8–20.3 LT, and then the eastward motions are dominant. The altitudinal variation of the zonal plasma motion is not significant. The plumes at 20.0–20.5 LT and 20.8–21.2 LT are developed above a horizontal backscatter layer which is considered to be produced by the electron density irregularities in the bottomside *F* region. Although the ionosonde observations are not available on that day,

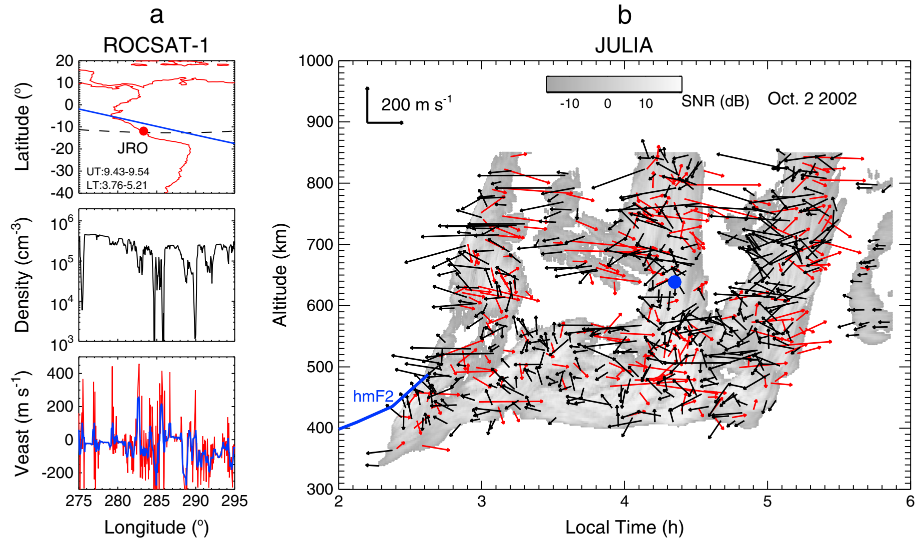

Figure 3. ROCSAT-1 and JULIA observations on 2 October 2002. (a) ROCSAT-1 orbit, plasma density, and zonal plasma velocity. (b) JULIA observations of the plasma velocity. The westward and eastward plasma motions are distinguished by the black and red arrows, respectively. The hmF2 is shown by a thick blue line. The magnetic apex height of ROCSAT-1 orbit is shown by a blue dot.

our observations on other days clearly show that the backscatter layer below plumes is located below the *F* peak height (hmF2). Here we emphasize the similarity of the turbulent zonal plasma motions inside plumes and in the bottomside backscatter layer. For the plume at 20.0–20.5 LT, the westward and eastward motions are mixed. On the other hand, eastward motion is dominant inside the plume at 20.8–21.2 LT. The difference of the plasma motions in the two plumes is consistent with the difference of the plasma motions in the bottomside backscatter layer at those intervals. The similarity of the plasma motions in the bottomside layer and plumes is also visible in the observations on 2 January 2002 (Figure 2b) and 16 September 2002 (Figure 2c). The hmF2 values derived from the ionosonde observations at JRO are shown by thick blue curves. As described above, the horizontal backscatter layers are located below the hmF2.

Figure 3 presents the ROCSAT-1 and JULIA observations at postmidnight on 2 October 2002. The ROCSAT-1 orbit and the measurements of the plasma density and zonal plasma velocity are shown in Figure 3a. The fluctuations of the zonal plasma velocities are significant inside bubbles, but their motions relative to ambient plasmas are not systematically westward or eastward. The JULIA observations of the backscatter power and plasma velocities are shown in Figure 3b. The westward and eastward velocities are shown with black and red arrows, respectively. The ROCSAT-1 orbit at the time of the pass over JRO is indicated by a blue dot. On average, the numbers of black and red arrows are similar inside plumes, although westward and eastward drifting tendencies exist in some local regions. The mixed zonal plasma motions inside plumes are consistent with the ROCSAT-1 observation. The hmF2 derived from ionosonde observations is shown with a blue line. Considering only a minor modulation of the height of the backscatter layer in the bottomside, hmF2 may maintain about 500 km between 2.5 and 5.0 LT. The turbulent zonal plasma motions do not show any notable difference between the regions below and above the estimated hmF2.

2.2. Comparison of the ROCSAT-1 and ISR observations

The coincident ROCSAT-1 and ISR observations of a bubble occurred at premidnight on 18 September and 13 December in 2001. Figure 4 is the same format as Figure 3 for the (a) ROCSAT-1 and (b) ISR observations on 18–19 September 2001. In the ROCSAT-1 observations, the zonal motion of the background ionosphere is eastward with an average velocity of ~150 m s^{-1}. Inside the bubble detected over JRO in Figure 4a, the plasma motions relative to the background plasmas are eastward at the west (left) side and westward at the east (right) side of the bubble. Because the ROCSAT-1 crossing time of the bubble is short (~50 s), the variation of the zonal velocity along the ROCSAT-1 orbit is interpreted as a spatial variation. In the ISR observations, the westward and eastward velocities are shown by black and white arrows, respectively.

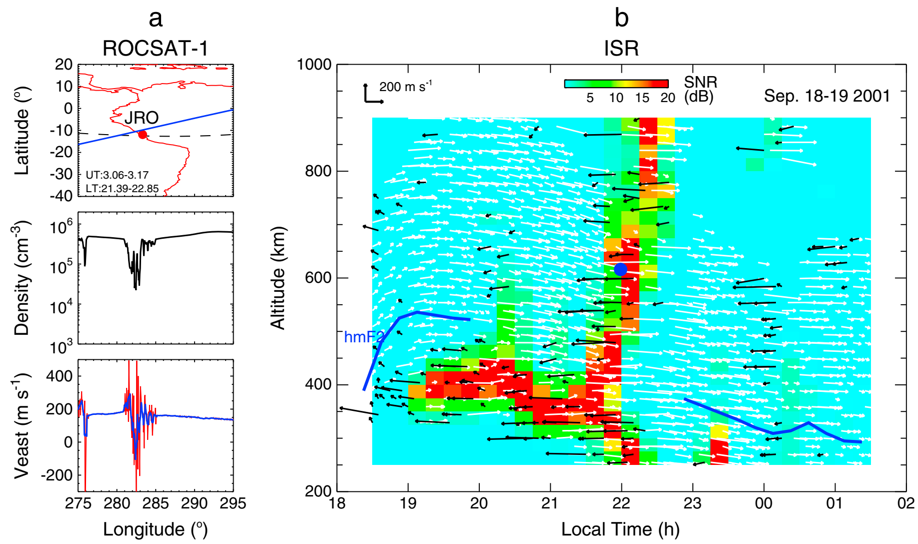

Figure 4. ROCSAT-1 and ISR observations on 18–19 September 2001. (a) ROCSAT-1 orbit, plasma density, and zonal plasma velocity. (b) ISR observations of backscatter power and plasma motion. The westward and eastward plasma motions are distinguished by the black and white arrows, respectively. The hmF2 is shown by a thick blue line. The magnetic apex height of ROCSAT-1 orbit is shown by a blue dot.

The ROCSAT-1 orbit is marked by a blue dot and the hmF2 is shown with a thick blue line. The hmF2 reaches the peak height (~540 km) at 19 LT and then decreases with time. This observation is consistent with the downward plasma motions after 19 LT. Ignoring the black arrows, eastward plasma flow exists all over the ionosphere. The plasma motions are not precisely divided by the topside and bottomside; the plasma flow just below hmF2 is the same as that in the topside. The black arrows (westward motions) appear mostly in the regions where the backscatter power is strong. In other words, the westward flow is a characteristic of the coherent backscatter region. Inside the plume, the westward flow is significant in the left side, but the flow is eastward in the right side with a greater velocity than the velocities of ambient plasmas. These properties exist in the bottomside backscatter layer where the plume originates. The opposite flows inside the plume are consistent with the plasma velocities inside the bubble detected by ROCSAT-1. Note that the left and right sides of the plume in Figure 4 correspond to the east and west sides of the bubble, respectively, when the *x* axis is changed from time to longitude. Using the eastward velocity (~150 m s^{-1}) of the background ionosphere observed by ROCSAT-1, the tilt angle of the plume detected around 22 LT is about 45°. Although the tilt of the plume in Figure 4b is much more significant than the tilts of the plumes in Figure 1c, the zonal plasma motions inside plumes do not show any notable dependence on the tilt angle.

Figure 5 is the same format as Figure 4 for the ROCSAT-1 and ISR observations on 13–14 December 2001. In the measurements of the zonal plasma velocity by ROCSAT-1 (Figure 5a), the drift of the background ionosphere is eastward. The plasmas inside bubbles, including the bubble detected over JRO, do not show a systematic westward or eastward motion relative to the background ionosphere. These observations are consistent with the plasma motions in the ISR observations in Figure 5b. Similar to the observations in Figure 4, the eastward flow exists in the whole ionosphere and the westward plasma motions appear mostly in the regions where the backscatter power is strong. The hmF2 is about 500 km at 20 LT. The vertical plasma motion is upward until 22 LT, near zero between 22 and 23 LT, and downward after 23 LT. By using those vertical plasma flows and the hmF2 before 20 LT, hmF2 is estimated to reach an altitude of 600 km at 22–23 LT and then decreases to about 400 km at 01 LT. For the eastward flow (white arrows), the plasma velocity increases after ~20 LT and then decreases after ~23 LT. For the westward flow (black arrows), the plasma velocities before ~22 LT are greater than those after ~22 LT. These variations appear both below and above the estimated hmF2. The ISR observations again demonstrate that the zonal plasma motions inside plumes resemble those in the bottomside backscatter layer.

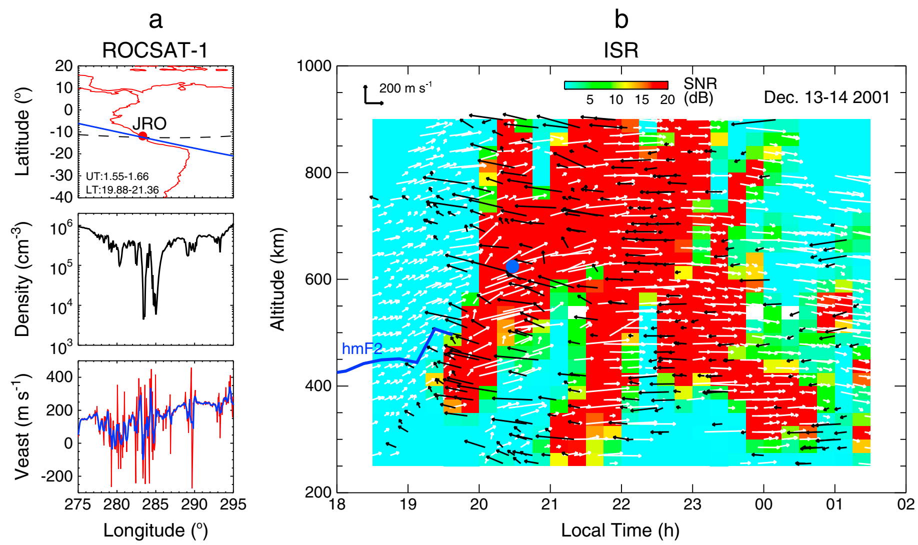

Figure 5. ROCSAT-1 and ISR observations on 13–14 December 2001. (a) ROCSAT-1 orbit, plasma density, and zonal plasma velocity. (b) ISR observations of backscatter power and plasma motion. The westward and eastward plasma motions are distinguished by the black and white arrows, respectively. The hmF2 is shown by a thick blue line. The magnetic apex height of ROCSAT-1 orbit is shown by a blue dot.

3. Discussion

The vertical shear in the zonal plasma flow, characterized by the eastward flow in the topside and westward flow in the bottomside, exists at premidnight [*Kudeki et al.*, 1981; *Tsunoda et al.*, 1981]. The combination of the zonal shear flow with the prereversal enhancement [*Fejer et al.*, 1991] produces a vortex flow in the clockwise direction when the equatorial ionosphere is viewed northward. This phenomenon is explained by the *F* region dynamo driven by neutral winds [*Eccles et al.*, 1999; *Haerendel et al.*, 1992; *Kudeki and Bhattacharyya*, 1999]. In the ISR observations reported in early studies [e.g., *Kudeki and Bhattacharyya*, 1999], the vertical and zonal motions of plasmas in the topside are systematic, whereas those in the bottomside backscatter layer are turbulent regardless of the existence of plumes in the topside. Those properties also appear in our ISR observations. Bubbles detected in the topside are produced by the transport of plasmas in the bottomside. If the plasma motions in the bottomside and topside are different and those transported plasmas from the bottomside maintain the bottomside plasma motions, then the motions of plasmas inside a bubble deviate from those of ambient plasmas. This interpretation is supported by the observations of similar turbulent plasma motions inside bubbles and in the bottomside backscatter layer where the bubbles originate.

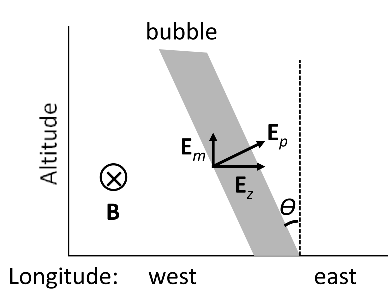

Figure 6. Schematic illustration of the polarization electric field inside a westward tilted bubble. According to *Huang et al.* [2010], the polarization electric field ($\mathbf{E}_p$) is perpendicular to the envelope of a bubble inside the bubble (gray region). The vertical ($\mathbf{E}_m$) and eastward ($\mathbf{E}_z$) components of $\mathbf{E}_p$ drive the westward and upward drifts of plasmas inside the bubble.

As the radar and satellite observations show, significant difference exists between the zonal velocities of plasmas inside and outside bubbles, although the tilts of bubbles are minor. These observations contradict the hypothesis proposed by *Huang et al.* [2010]. According to *Huang et al.* [2010], the polarization electric field ($\mathbf{E}_p$) develops perpendicular to the envelope of a bubble due to the density gradient. The schematic diagram in Figure 6 illustrates the tilt of a bubble (gray region) and the direction of $\mathbf{E}_p$ in the longitude and altitude frame. The diagram is the view of the equatorial plane from the south. The direction of the magnetic field is northward (into the paper). The tilt angle of the plume is given by θ. Plasmas in the *F* region move perpendicular to the applied electric field (**E**) and magnetic field (**B**) (i.e., $\mathbf{E} \times \mathbf{B}$ drift), and therefore, the upward (V_m) and westward (V_z) plasma motions are driven by the eastward component ($\mathbf{E}_z$) and upward component ($\mathbf{E}_m$) of $\mathbf{E}_p$, respectively. The relationship between the two velocity components is given by $|V_z| = |V_m| \tan\theta$. In all of our radar and satellite observations, the average magnitudes of the fluctuations in the zonal velocities were greater than those in the vertical velocities inside plumes. Substantial tilt angles are required to explain those observations by the effect of the tilt. However, the large westward plasma motions at the bubbles of small tilt angles are not explained by the effect of the polarization electric field. In our observations, the average eastward velocities of plasmas inside bubbles are smaller than those of ambient plasmas. The smaller eastward velocity inside bubbles can be caused by either an overall reduction of the eastward velocity or the existence of westward drifting plasmas. If the vertical component of the polarization electric field were responsible for the reduced eastward velocity, its effect would appear as a systematic reduction of the eastward velocity. However, our observations show that the reduced eastward velocities inside bubbles are not caused by the systematic reduction of the eastward velocities; it is primarily due to the existence of westward drifting plasmas. The mixture of the westward and eastward plasma motions in random fashion is difficult to explain by the effect of the polarization electric field.

Huang et al. [2010] claimed that the westward motions of plasmas inside a westward tilted bubble make the envelope of a bubble drift eastward faster than the background because the plasmas at the east envelope are transported to west. Following this hypothesis, the motions of plasmas inside a bubble are opposite to the motion of the envelope. With an increase of the westward tilt angle, the plasmas at the east envelope move westward faster. As a result, the eastward drift of the envelope relative to the background ionosphere becomes faster with an increase of the westward tilt angle. Before we discuss the motion of the envelope of a bubble, let us think about the definition of the envelope. The envelope may be considered to be the walls that confine plasma depletions or turbulence. These walls are formed by the background plasmas. The polarization electric field is effective inside the envelope, but it is not on the envelope. Otherwise, the plasmas on the envelope will also be lifted and the region on the envelope will be depleted. Because the envelope does not belong to a bubble, its movement represents the motion of the background ionosphere. When an optical imager observes the zonal drift of a bubble, its observation is the movement of the envelope. The zonal drift velocity of a bubble derived from scintillation observations can also be considered to be the drift velocity of the envelope because the correlation time of the scintillation patterns at spaced receivers is related to the zonal drift of the irregularity structure rather than the motion of individual plasmas. Thus, the bubble velocities derived from those observations represent the motions of the background ionosphere.

The plasmas inside bubbles can be considered trapped plasmas by high-density ambient plasmas (or envelope). The trapped plasmas maintain their turbulent motions inside the envelope, but their bulk motion is carried by the envelope. Therefore, as the radar and in situ observations show, the velocities of the plasmas inside bubbles and of ambient plasmas can be different. As time progresses, collisions between the trapped plasmas and ambient plasmas reduce the difference. So, the difference may depend on LT as well as the zonal plasma motions in the bottomside and topside.

4. Conclusions

We have investigated the plasma motions inside bubbles and the drift of bubbles relative to the bubble-embedded background ionosphere using the simultaneous ROCSAT-1 and radar (ISR and JULIA) observations over JRO. In the ROCSAT-1 observations at premidnight, plasmas inside bubbles show westward drifts relative to ambient plasmas regardless of the tilt of bubbles.

The observations of the relative westward drifts inside bubbles of small tilt angles indicate that the tilt is not the primary cause of the deviation of the zonal plasma motions inside bubbles. The nighttime zonal plasma motions are characterized by a systematic eastward drift in the topside. However, the zonal plasma motions in the region where the coherent backscattering occurs are a mixture of the eastward and westward motions. The similarity of the plasma motions inside plumes and in the bottomside backscatter layer indicates that the plasma motions inside bubbles maintain the properties of the plasma motions in the bottomside backscatter layer where the bubbles originate. On the basis of these observations, we interpret the deviation of the motions of plasmas inside bubbles from those of ambient plasmas in terms of the difference of the plasma flows in the bottomside and topside.

Acknowledgments
H. Kil acknowledges support from National Science Foundation Aeronomy program (AGS-1237276). Y.-S. Kwak acknowledges support by a grant from the U.S. Air Force Research Laboratory, under agreement FA 2386-14-1-4004 and by the "Study of near-Earth effects by CME/HSS" project from Korea Astronomy and Space Science Institute. The Jicamarca Radio Observatory is a facility of the Instituto Geofísico del Perú operated with support from National Science Foundation Cooperative agreement AGS-0905448 through Cornell University. The radar and ionosonde data for this paper are available at the CEDAR Madrigal Database (http://cedar.openmadrigal.org) and UMLCAR website (http://ulcar.uml.edu/DIDBase). The ROCSAT-1 data are available by contacting H. Kil.

Alan Rodger thanks the reviewers for their assistance in evaluating the paper.

References

Abdu, M. A., I. J. Kantor, I. S. Batista, and E. R. de Paula (1985), East–west plasma bubble irregularity motion determined from spaced VHF polarimeter: Implications on velocity shear in the zonal *F* region bulk plasma motion, *Radio Sci.*, *20*, 111–122, doi:10.1029/RS020i001p00111.

Abdu, M. A., J. H. A. Sobral, Y. Nakamura, and C. J. Zamlutti (1987), Equatorial plasma bubble zonal velocity height gradient from spaced VHF polarimeter and scanning 630-nm measurements, *Geophys. Res. Lett.*, *14*, 965–968, doi:10.1029/GL014i009p00965.

Basu, S., and S. Basu (1981), Equatorial scintillations—A review, *J. Atmos. Sol. Terr. Phys.*, *43*, 473–489.

Basu, S., S. Basu, E. Kudeki, H. P. Zengingonul, M. A. Biondi, and J. W. Meriwether (1991), Zonal irregularity drifts and neutral winds measured near the magnetic equator in Peru, *J. Atmos. Sol. Terr. Phys.*, *53*, 743–755.

Basu, S., et al. (1996), Scintillations, plasma drifts, and neutral winds in the equatorial ionosphere after sunset, *J. Geophys. Res.*, *101*, 26,795–26,809, doi:10.1029/96JA00760.

Bhattacharyya, A., S. Basu, K. M. Groves, C. E. Valladares, and R. Sheehan (2001), Dynamics of equatorial *F* region irregularities from spaced receiver scintillation observations, *Geophys. Res. Lett.*, *28*, 119–122, doi:10.1029/2000GL012288.

Coley, W. R., and R. A. Heelis (1989), Low-latitude zonal and vertical ion drifts seen by DE2, *J. Geophys. Res.*, *94*, 6751–6761, doi:10.1029/JA094iA06p06751.

de Paula, E. R., M. T. A. H. Muella, J. H. A. Sobral, M. A. Abdu, I. S. Batista, T. L. Beach, and K. M. Groves (2010), Magnetic conjugate point observations of kilometer and hundred-meter scale irregularities and zonal drifts, *J. Geophys. Res.*, *115*, A08307, doi:10.1029/2010JA015383.

Eccles, J. V., N. Maynard, and G. Wilson (1999), Study of the evening plasma drift vortex in the low-latitude ionosphere using San Marco electric field measurements, *J. Geophys. Res.*, *104*, 28,133–28,143, doi:10.1029/1999JA900373.

Fejer, B. G., E. R. de Paula, S. A. González, and R. F. Woodman (1991), Average vertical and zonal *F* region plasma drifts over Jicamarca, *J. Geophys. Res.*, *96*, 13,901–13,906, doi:10.1029/91JA01171.

Fejer, B. G., E. R. de Paula, R. A. Heelis, and W. B. Hanson (1995), Global equatorial ionospheric vertical plasma drifts measured by the AE-E satellite, *J. Geophys. Res.*, *100*, 5769–5776, doi:10.1029/94JA03240.

Fejer, B. G., J. W. Jensen, and S.-Y. Su (2008), Quiet time equatorial *F* region vertical plasma drift model derived from ROCSAT-1 observations, *J. Geophys. Res.*, *113*, A05304, doi:10.1029/2007JA012801.

Haerendel, G., J. V. Eccles, and S. Çakir (1992), Theory for modeling the equatorial evening ionosphere and the origin of the shear in the horizontal plasma flow, *J. Geophys. Res.*, *97*, 1209–1223, doi:10.1029/91JA02226.

Huang, C.-S., O. de La Beaujardiere, R. F. Pfaff, J. M. Retterer, P. A. Roddy, D. E. Hunton, Y.-J. Su, S.-Y. Su, and F. J. Rich (2010), Zonal drift of plasma particles inside equatorial plasma bubbles and its relation to the zonal drift of the bubble structure, *J. Geophys. Res.*, *115*, A07316, doi:10.1029/2010JA015324.

Hysell, D. L., and J. D. Burcham (1998), JULIA radar studies of equatorial spread *F*, *J. Geophys. Res.*, *103*, 29,155–29,167, doi:10.1029/98JA02655.

Immel, T. J., S. B. Mende, H. U. Frey, L. M. Peticolas, and E. Sagawa (2003), Determination of low latitude plasma drift speeds from FUV images, *Geophys. Res. Lett.*, *30*(18), 1945, doi:10.1029/2003GL017573.

Kelley, M. C. (1989), *The Earth's Ionosphere*, Academic Press, San Diego, Calif.

Kil, H., P. M. Kintner, E. R. de Paula, and I. J. Kantor (2000), Global positioning system measurements of the ionospheric zonal apparent velocity at Cachoeira Paulista in Brazil, *J. Geophys. Res.*, *105*, 5317–5327, doi:10.1029/1999JA000244.

Kil, H., P. M. Kintner, E. R. de Paula, and I. J. Kantor (2002), Latitudinal variations of scintillation activity and zonal plasma drifts in South America, *Radio Sci.*, *37*(1), 1006, doi:10.1029/2001RS002468.

Kil, H., S.-J. Oh, L. J. Paxton, and T.-W. Fang (2009), High-resolution vertical drift model driven from the ROCSAT-1 data, *J. Geophys. Res.*, *114*, A10314, doi:10.1029/2009JA014324.

Kudeki, E., and S. Bhattacharyya (1999), Postsunset vortex in equatorial *F* region plasma drifts and implications for bottomside spread *F*, *J. Geophys. Res.*, *104*, 28,163–28,170, doi:10.1029/1998JA900111.

Kudeki, E., B. G. Fejer, D. T. Farley, and H. M. Ierkic (1981), Interferometer studies of equatorial *F* region irregularities and drifts, *Geophys. Res. Lett.*, *8*, 377–380, doi:10.1029/GL008i004p00377.

Liu, G., S. L. England, H. U. Frey, T. J. Immel, C. S. Lin, E. E. Pacheco, K. Häusler, and E. Doornbos (2013), Comparison of drift velocities of nighttime equatorial plasma depletions with ambient plasma drifts and thermospheric neutral winds, *J. Geophys. Res. Space Physics*, *118*, 7360–7368, doi:10.1002/2013JA019329.

Makela, J. J. (2006), A review of imaging low-latitude ionospheric irregularity processes, *J. Atmos. Sol. Terr. Phys.*, *68*, 1441–1458, doi:10.1016/j.jastp.2005.04.014.

Martinis, C., J. V. Eccles, J. Baumgardner, J. Manzano, and M. Mendillo (2003), Latitude dependence of zonal plasma drifts obtained from dualsite airglow observations, *J. Geophys. Res.*, *108*(A3), 1129, doi:10.1029/2002JA009462.

Park, S. H., S. L. England, T. J. Immel, H. U. Frey, and S. B. Mende (2007), A method for determining the drift velocity of plasma depletions in the equatorial ionosphere using far ultraviolet spacecraft observations, *J. Geophys. Res.*, *112*, A11314, doi:10.1029/2007JA012327.

Scherliess, L., and B. G. Fejer (1999), Radar and satellite global equatorial *F* region vertical drift model, *J. Geophys. Res.*, *104*, 6829–6842, doi:10.1029/1999JA900025.

Sobral, J. H. A., and M. A. Abdu (1990), Latitudinal gradient in the plasma bubble zonal velocities as observed by scanning 630-nm airglow measurements, *J. Geophys. Res.*, *95*, 8253–8257, doi:10.1029/JA095iA06p08253.

Sultan, P. J. (1996), Linear theory and modeling of the Rayleigh-Taylor instability leading to the occurrence of equatorial spread *F*, *J. Geophys. Res.*, *101*, 26,875–26,891, doi:10.1029/96JA00682.

Tsunoda, R. T., R. C. Livingston, and C. L. Rino (1981), Evidence of a velocity shear in bulk plasma motion associated with the post-sunset rise of the equatorial *F*-layer, *Geophys. Res. Lett.*, *8*, 807–810, doi:10.1029/GL008i007p00807.

Valladares, C., R. Sheehan, S. Basu, H. Kuenzler, and J. Espinoza (1996), The multi-instrumented studies of equatorial thermosphere aeronomy scintillation system: Climatology of zonal drifts, *J. Geophys. Res.*, *101*, 26,839–26,850, doi:10.1029/96JA00183.

Woodman, R. F., and C. La Hoz (1976), Radar observations of *F* region equatorial irregularities, *J. Geophys. Res.*, *81*, 5447–5466, doi:10.1029/JA081i031p05447.

Yeh, H. C., S.-Y. Su, R. A. Heelis, and J. M. Wu (1999), The ROCSAT-1 IPEI preliminary results: Vertical ion drift statistics, *Terr. Atmos. Oceanic Sci.*, *10*, 805–820.

